

Laboratory evaluation of a novel thermal dissociation chemiluminescence method for in situ detection of nitrous acid

Idalia M. Pérez^a, Paul J. Wooldridge^a, Ronald C. Cohen^{a,b,c,*}

^aDepartment of Chemistry, University of California, Berkeley, CA 94720, USA

^bDepartment of Earth and Planetary Sciences, University of California, Berkeley, CA 94720, USA

^cEnergy and Environment Technologies Division, Lawrence Berkeley National Laboratory,
1 Cyclotron Road MS Latimer, Berkeley, CA, USA

Received 9 May 2006; received in revised form 19 December 2006; accepted 17 January 2007

Abstract

We describe a new laboratory-based method for in situ detection of nitrous acid (HONO) using a combination of thermal dissociation (TD) and chemiluminescent (CL) detection of nitric oxide. A prototype was built using a commercial NO sensor. Laboratory tests for possible chemical interferences show that measurements are affected in predictable ways by NO₂, peroxy nitrates, alkyl nitrates, HNO₃, O₃ and H₂O.

© 2007 Elsevier Ltd. All rights reserved.

Keywords: Nitrous acid; Instrument; Nitrogen oxides; HONO

1. Introduction

Nitrous acid, HONO, has been recognized as an important contributor to atmospheric HO_x production (Alicke et al., 2002, 2003; Aumont et al., 2003; Ren et al., 2003; Kleffmann et al., 2005) and may represent as much as 13% of the atmospheric reactive nitrogen reservoir (Zhou et al., 2002a). Although the mechanism for HONO production remains elusive and controversial (e.g. Finlayson-Pitts et al., 2003), field measurements are providing evidence for the presence of HONO in a range of urban, rural and remote locations (e.g. Honrath

et al., 2002; Zhou et al., 2002a; Stutz et al., 2004). An improved understanding of the mechanisms controlling HONO concentrations will require measurements of HONO in concert with a full suite of other HO_x and NO_y species, measurements of HONO fluxes and measurements of vertical gradients in HONO concentration.

Most prior measurements of HONO in the atmosphere have been based on wet chemical methods or on long path absorption spectroscopy. Wet chemical sampling with derivatization followed by HPLC separation (e.g. Zhou et al., 1999) and UV detection (e.g. Heland et al., 2001) and direct sampling with denuders or filters followed either by ion chromatography (e.g. Ferm and Sjödin, 1985; Večeřa and Dasgupta, 1991; Simon and Dasgupta, 1995; Oms et al., 1996; Zellweger et al., 1999; Genfa et al., 2003; Bytnerowicz et al., 2005) or

*Corresponding author. Department of Chemistry, University of California, Berkeley, CA 94720, USA. Tel.: +1 510 642 2735; fax: +1 510 643 2156.

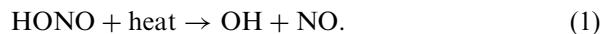
E-mail address: cohen@cchem.berkeley.edu (R.C. Cohen).

by derivatization and fluorescent detection (Take-naka et al., 2004) have been used extensively. The integration time for wet sampling or filter sampling techniques spans from a few minutes up to weeks. Heland et al. (2001) report detection limits of 3–6 ppt with a 4 min integration time and Beine et al. (2005) report detection limits of 0.5 ppt with an integration time of 5 min. Bytnerowicz et al. (2005) describe a passive sampling method for measuring HONO that is intended for integrating over extended periods of time, usually 1–4 weeks. HONO has also been detected directly using differential optical absorption spectroscopy (e.g. Alicke et al., 2002) with detection limits of 84 ppt (Alicke et al., 2003). Laser-induced detection of the OH fragment following the photofragmentation of HONO with a sensitivity of 10 ppt in 5 min has also been developed (Liao et al., 2006). Cavity ring-down spectroscopy has also been proposed as a method for HONO detection (Wang and Zhang, 2000) but has not been used for field measurements to our knowledge.

We propose a new strategy for HONO detection based on thermal dissociation (TD) coupled to chemiluminescent (CL) detection of NO (TD-CL). The method has the potential to provide an order of magnitude higher time resolution than any of the above techniques with comparable detection limits. We describe laboratory tests of the proposed design and evaluate factors affecting the instrument response and potential interferences. Modifications to the prototype are proposed that will improve the instrument's prospects for successful field measurements.

2. Thermal dissociation—chemiluminescence detection of HONO

In recent work, Day et al. (2002) show the use of gas phase TD of peroxy nitrates (Σ PNs), alkyl nitrates (Σ ANs) and nitric acid (HNO_3) followed by the detection of the NO_2 fragment by LIF is an accurate and sensitive method for detection of these species. We follow a similar strategy for the detection of HONO. Upon heating, HONO molecules thermally dissociate to yield NO and OH (Fig. 1)



The NO fragment is then detected using the CL reaction with O_3 . Commercial instruments for NO detection with sensitivities of 50 ppt in 3 s or 10 ppt

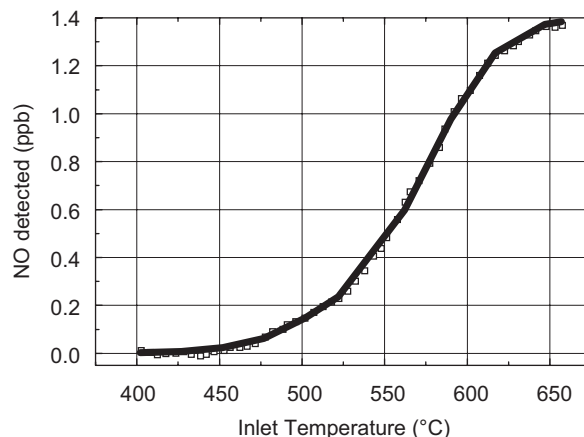


Fig. 1. Nitric oxide detected by chemiluminescence during a temperature ramp (400–670 °C) of 1.39 ppb of nitrous acid in zero air along with a model temperature ramp. The model used to produce this figure is discussed below.

in 60 s (Eco Physics, CLD 780 TR) are available and designs with sensitivities of 1–2 ppt in 10 s have been developed (e.g. Ridley and Grahek, 1990). Sensitive and accurate detection of HONO requires three additional elements: an inlet, a method of calibration, and a method of accounting for secondary chemistry affecting the amount of NO arriving at the detection region. These three elements are described below.

2.1. Inlet

We use an inlet similar to the one described by Day et al. (2002). Air is taken in through a $\frac{1}{4}$ in (6.4 mm) OD quartz tube and is rapidly heated, producing an enhancement in NO over the ambient background. In our laboratory experiments we used a two-channel system which sampled air at approximately 2 standard liters per minute through 15 cm of PFA tubing heated to approximately 50 °C to prevent losses of HONO to the walls of the inlet and then split into two equal flows directed through a 120 cm long section of 6.4 mm OD (3.8 mm ID) long quartz tubing (see Fig. 2). The first channel is set at ambient temperature and is used to measure NO and the second channel is heated to the temperature at which HONO dissociated (640 °C) and used to measure the sum of NO and HONO. Nichrome wire wrapped around the first 25 cm of the quartz tubing resistively heats that segment and the remaining \sim 100 cm is used to cool the gas. Quartz tubing surrounds the heated section to

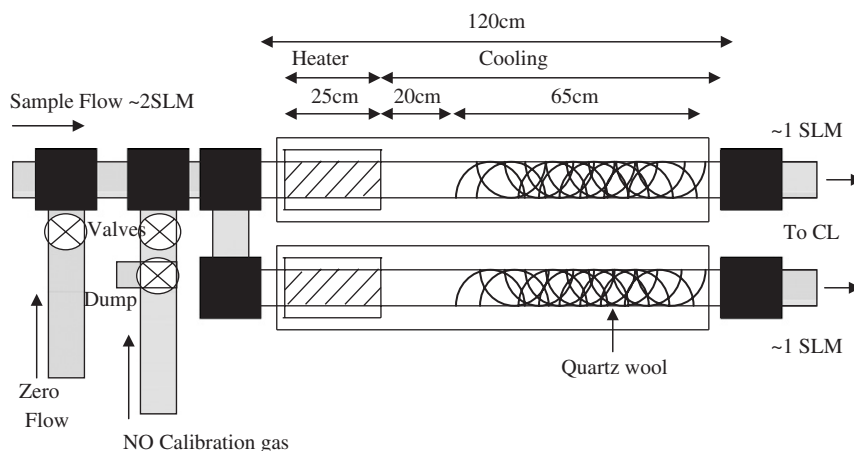


Fig. 2. Diagram of inlet.

protect the Nichrome and acts as insulation. A thermocouple attached to the quartz tubing is used as a feedback for temperature control. After cooling, the gas enters 6.4 mm OD (3.8 mm ID) PFA tubing that transports the sample to the detector. At residence times of about 30 ms and a pressure of 1 atm, HONO thermally dissociates to produce NO at 640 °C. The temperatures used in this paper are defined operationally, based on the experimental temperature ramp of HONO (cf. Fig. 1) where the temperatures are measured with the thermocouple mentioned above and do not correspond to the actual temperatures of the gas. Calculations show the gas temperature required for complete dissociation of HONO in 30 ms is 680 °C.

To decrease the concentration of OH and peroxy radicals ($RO_2 = RO_2 + HO_2$) produced in the heated section of the inlet, and thus minimize the subsequent secondary chemistry, quartz wool was placed 20 cm downstream of the heated section. This added surface area increases the loss of reactive radicals without affecting the NO concentration. Inlets both with and without the quartz wool were tested as described in Section 2.3 and we conclude that, as long as the quartz wool is well downstream of the heated section, it is an effective scavenger of radicals. All of the results described below were obtained using quartz wool in the inlet.

At the front end of the PFA inlet, before the heaters, two PFA swagelock tees are incorporated where an NO standard and zero air are injected for calibration. Solenoid valves prevent the calibration gas and zero air from entering the instrument when sampling.

2.2. Calibration

We assessed the behavior of HONO in the instrument and characterized its conversion efficiency by comparison with a commercial NO/NO_y instrument (Thermo Environmental Co. 42CTL) that uses a Mo converter set at 350 °C to convert HONO (and other NO_y species) to NO. NO chemiluminescence detectors with Mo converters set a 350 °C have been shown to have near unit response to HONO (Allegrini et al., 1990). This instrument was calibrated with NO (5.42 ppm ± 5% in N₂, Praxair Inc.) and the conversion efficiency was tested using NO₂ (4.63 ppm NO₂, 0.1 ppm NO in N₂, Praxair Inc.) and a HNO₃ standard prepared using a homebuilt permeation device (2.4 ppb in our zero air flow rate). The background was measured using zero air (Sabio Instrument Inc., 1001/1000M).

HONO was generated by flowing a H₂SO₄ aerosol through NaNO_{2(s)} dispersed between filters (50 μm PTFE):



Aerosol was produced by disrupting the surface of an approximately 0.5 M H₂SO_{4(aq)} with a stream of nitrogen gas (800–1200 sccm) aimed at the surface of the solution. This mixture was diluted with zero air to produce HONO mixing ratios of 1–3 ppb. Fig. 3 shows 2 h of output from the source as measured by the TD-CL. The mean concentration was 1.11 ppb with a standard deviation of 0.06 ppb. A similar technique for producing HONO was described by Bertman et al. (2003) using NaNO₂ between paper filters and flowing HNO₃

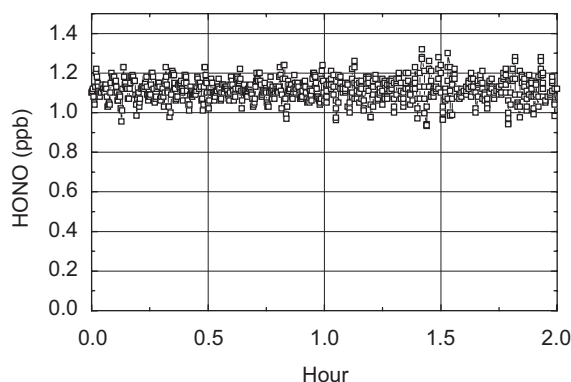
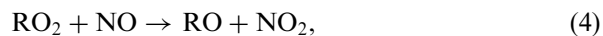
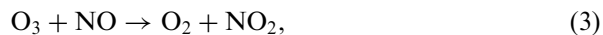


Fig. 3. Time series of HONO produced as described in text and measured using TD-CL.

through the filters. In our work, H_2SO_4 was used instead of HNO_3 because of the possibility of HNO_3 interfering with our measurement. We initially tried a calibration source based on the reaction of $\text{HCl}_{(\text{g})}$ with NaNO_2 as described by Febo et al. (1995), but identified trace quantities of ClNO in this source. The ClNO was observed to dissociate at 450°C producing NO . Using H_2SO_4 aerosol to react with $\text{NaNO}_{2(\text{s})}$ we observed only NO and a signal appearing at an inlet temperature consistent with HONO dissociating. The purity of the HONO generated with the H_2SO_4 was examined using TD with LIF detection of NO_2 (Day et al., 2002). No NO_2 containing compounds were observed. Taken together these experiments show that the HONO source had a purity of at least 95% with the major impurity being NO .

2.3. Secondary chemistry

Day et al. (2002) and Rosen (2004) discussed several possible effects that could complicate the interpretation of measurements of NO or NO_2 using the TD technique. These include NO oxidation by RO_2 and O_3 as well as the reduction of NO_2 by O atoms:



In the heated inlet, at temperatures above 225°C , O_3 dissociates into molecular oxygen very quickly minimizing the importance of the reaction of O_3

with NO (reaction (3)).



The O atom formed in the inlet reacts almost exclusively with water leading to elevated concentrations of OH , which after reacting with hydrocarbons, lead to RO_2 mixing ratios that are much higher than ambient mixing ratios.

We constructed a kinetic model representing the chemistry that occurs in the inlet. The model, which describes the different sections of the inlet including relevant temperatures and residence times, includes the above reactions (1), (3)–(6) as well as other relevant reactions (see Tables 1–4 in the supplementary information section). Loss of OH and O radicals onto walls (k_{wall}) are calculated based on their diffusion to the wall and assuming an uptake coefficient of unity (Gormley and Kennedy, 1949). The approximate probability that a molecule will encounter the quartz wool was determined using a collision frequency based on the pressure and temperature of the gas as well as an approximate surface area along the length of the quartz wool. For ease of calculation, reactions in which molecular oxygen is one of the reactants and thus occurring orders of magnitude faster than other reactions were assumed to happen instantly and were eliminated from the explicit calculation.

At 640°C , all XONO and XONO_2 , where X is H , R or RO , species are completely dissociated to NO and NO_2 , respectively. The secondary chemistry described briefly above affects the total NO and NO_2 mixing ratios regardless of their original source (e.g. sources of NO_2 include peroxy nitrates, alkyl nitrates and HNO_3). Thus, we can study the effects of secondary chemistry in the laboratory with experiments that examine NO and NO_2 detection efficiencies under a variety of conditions. Additionally, the effect of the XONO_2 species is further discussed on the basis of model studies in Section 3.3. Organic nitrites, RONO , are not described in this text because their atmospheric concentration is expected to be negligible.

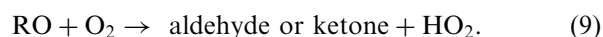
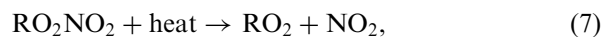
3. Laboratory tests

We characterized the NO detection efficiency over a range of CH_4 (1000–1700 ppb), O_3 (0–100 ppb), NO_2 (0–40 ppb) and water mixing ratios (10–80% relative humidity) confirming that the NO detection efficiency behaves as predicted by model

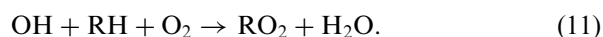
calculations. Similarly we characterized the conversion efficiency of NO₂ to NO over a wide range of conditions. For these studies, ozone was produced by photolysis of zero air at 185 nm using a mercury lamp and quantified using a commercial ozone instrument (2B Technologies Inc., Model 202). We dynamically diluted 4.63 ppm NO₂, 0.1 ppm NO in N₂, Praxair Inc. and 5.42 ppm ± 5% in N₂, Praxair Inc. standards. The CH₄ concentration was varied by using a zero air generator with or without a methane oxidizer (Sabio Instrument Inc., Model 1001/1000M). Model calculations show that the reactions of O with N₂O and O with NH₃ are not significant sources of NO under conditions we are using for HONO detection.

3.1. NO oxidation

The fraction of NO oxidized to NO₂ before detection is proportional to the concentration of oxidant available. For the TD-CL technique, there is an elevated mixing ratio of RO₂ in the heated channel due to three distinct processes that occur upon heating the sample. These include the dissociation of peroxy nitrates (ΣPNs) and alkyl nitrates (ΣANs):



In addition to these reactions, RO₂ is produced by the reaction of VOCs with OH, which is present in elevated concentrations due to the O + H₂O reaction:



The elevated OH mixing ratio is confined to the heated section of the inlet where the OH is rapidly converted to RO₂ primarily by reaction with methane at high temperatures. The mixing ratio of OH produced in the inlet by atomic oxygen reacting with water is much larger than the OH produced by HONO, HNO₃ and H₂O₂ dissociation. For example, in the heated inlet with an O₃ mixing ratio of 50 ppb and a relative humidity of 50% at 25 °C, we calculate a peak RO₂ mixing ratio of 7 ppb due to the sequence of reactions (6) and (10)–(11), but only 0.59 ppb due to direct OH production from HONO, HNO₃ or H₂O₂ dissociation (assuming 2 ppb of

each compound). With an O₃ mixing ratio of 100 ppb, the RO₂ mixing ratio increases to 11 ppb. This effect is not linear with O₃ because of the increasing importance of radical–radical loss processes at high RO₂ concentration. The mixing ratios of RO₂ due to reactions (7)–(9) are typically of order 1 ppb in rural settings and 2 ppb in urban settings.

Fig. 4 shows the observed and calculated fractions of NO detected when a mixture of 6.29 ppb of NO in zero air with a relative humidity of 10% and a CH₄ concentration of 1.7 ppm is exposed to different concentrations of O₃ (5–100 ppb) at 640 °C as well as the calculated fraction of NO detected at 80% relative humidity. As O₃ concentrations increase, radical–radical loss processes become increasingly important causing the nonlinear response of NO to O₃. At 100 ppb of O₃, 80% of the original NO is detected. Fig. 4 demonstrates that the oxidation of NO has a slight dependence on RH, such that at the highest concentration of ozone the detection efficiency is approximately 80% at 10% relative humidity and 77% at 80% relative humidity. At low O₃ concentrations, the humidity dependence is less important because we are in pseudo-first order regime with respect to atomic oxygen. At lower concentrations of CH₄, the oxidation decreases as expected due to a decrease in RO₂ formation. The model reproduces the laboratory observations of NO yield to within ±5%.

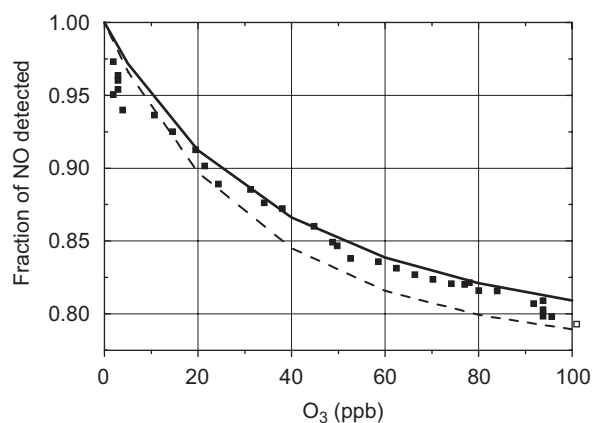


Fig. 4. Fraction of NO detected by TD-CL from a mixture of 6.29 ppb NO and O₃ (5–100 ppb) in zero air with methane (1.7 ppm) and a RH of 10% along with model results (solid line). Also shown are model results of the same mixture in zero air with a RH of 80% (dashed line).

3.2. NO₂ reduction

The reduction of NO₂ to NO that occurs in the inlet is due to its reaction with O atoms (reaction (5)) produced by dissociation of O₃ (reaction (6)) in the heated section of the inlet. In the absence of O₃ we observe no measurable conversion of NO₂ to NO; the dissociation temperature for NO₂ is approximately 1300 °C. Atomic oxygen can also react with water, VOCs and with the walls of the inlet. The fraction of atomic oxygen that reacts with NO₂ (F_{O+NO_2}) is given by

$$F_{O+NO_2}(T) = \frac{k_{O+NO_2}(T)[NO_2]}{k_{\text{wall}}(T) + k_{O+H_2O}(T)[H_2O] + k_{O+CH_4}(T)[CH_4] + k_{O+NO_2}(T)[NO_2]}, \quad (12)$$

where k_{O+H_2O} , k_{O+CH_4} and k_{O+NO_2} are rate constants for the reaction of the atomic oxygen with H₂O, CH₄ and NO₂, respectively, and k_{wall} is the rate constant for the loss of atomic oxygen to the wall. At high temperatures the O reaction with CH₄ dominates over its reaction with other hydrocarbons because of the much larger concentration of CH₄ present. Although the reaction of O with NO₂ does not have a steep temperature dependence between ambient temperature and 640 °C, O atom reactions with water and CH₄ do, thus F_{O+NO_2} decreases as temperature increases. Ozone dissociation in our inlet starts at 225 °C and is complete by 550 °C. This increase in atomic oxygen and the decrease in F_{O+NO_2} explain the behavior of the NO

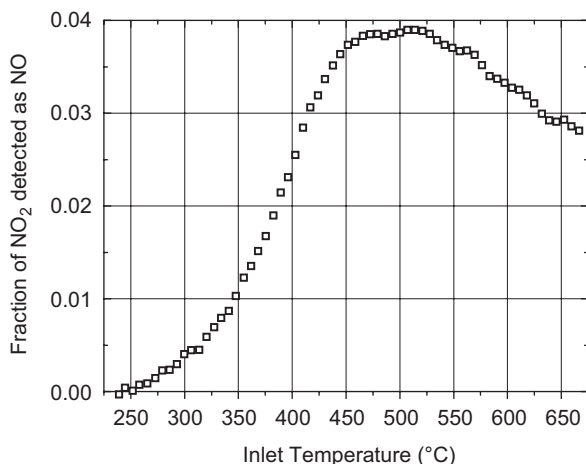


Fig. 5. Fraction of NO₂ detected as NO by chemiluminescence during a temperature ramp (225–675 °C) of 13.83 ppb of NO₂ in a mixture of zero air and 73 ppb of ozone.

signal as a function of temperature in the presence of O₃ and NO₂ shown in Fig. 5.

The NO signal in the presence of NO₂ at different concentrations of O₃ in zero air with a 10% RH and a CH₄ concentration of 1.7 ppm is shown in Fig. 6 along with the calculated NO detection efficiency at 10% and 80% RH. Oxygen atoms increase linearly with increasing ozone concentration explaining the linear response of NO to O₃ in the presence of NO₂. The experimental results show that at 100 ppb of O₃ approximately 4% of the total NO₂ available (NO₂ + ΣPNs + ΣANs + HNO₃) is converted to

NO. Experimental results not shown but accurately represented by the model curve in Fig. 6 demonstrate that at higher relative humidity with a CH₄ mixing ratio of 1.7 ppm, the observed NO₂ reduction due to ozone decreases because of the competition for O atoms by H₂O as well as because of an increase in re-oxidation of the NO formed from NO₂ due to an increase in RO₂.

3.3. Calculated performance of laboratory prototype

Fig. 7 shows calculations of the mixing ratio of NO expected at the detector as a function of temperature for a rural and an urban nighttime scenario, each with and without 100 ppt and 1.8 ppb

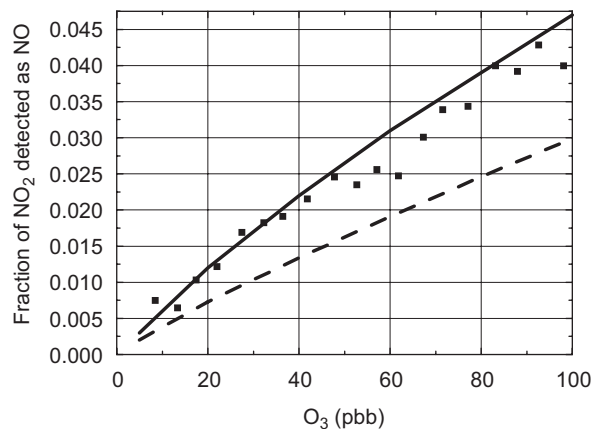


Fig. 6. Fraction of NO₂ detected as NO by TD-CL with the inlet set at 640 °C from a mixture of 21.3 ppb NO₂ and O₃ (10–100 ppb) in zero air with a RH of 10% along with model results (solid line). Also shown are model results of the same mixture in zero air with a RH of 80% (dashed line).

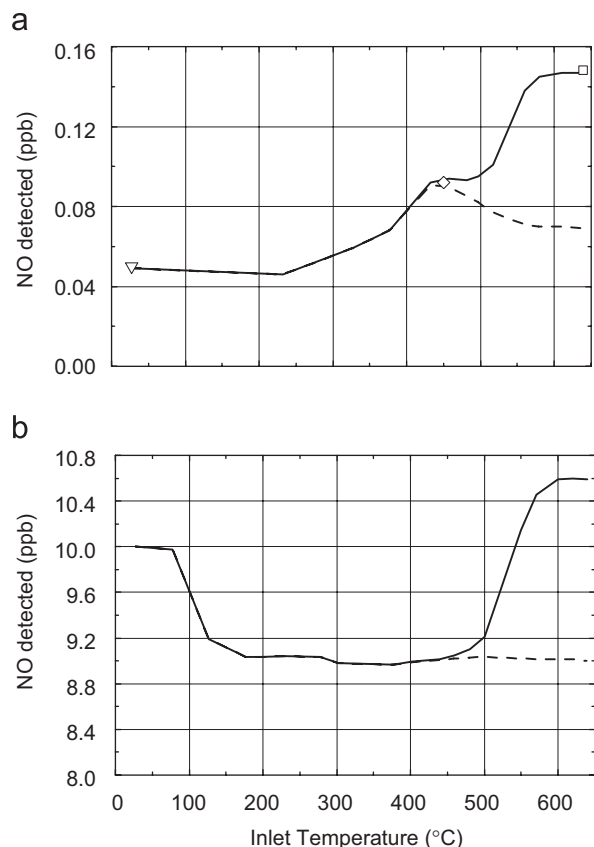


Fig. 7. Modeled temperature ramp (0–650 °C) of (a) a mixture of O_3 (50 ppb), NO (0.05 ppb), NO_2 (0.5 ppb), ΣPN_s (0.5 ppb), ΣAN_s (0.5 ppb) and HNO_3 (0.5 ppb) in ambient air with a RH of 50% with (solid line) and without (dashed line) HONO (0.1 ppb) and (b) a typical urban nighttime atmosphere where O_3 is fully titrated (0 ppb) with NO (10 ppb), NO_2 (60 ppb), ΣPN_s (2 ppb), ΣAN_s (2 ppb) and HNO_3 (2 ppb) in ambient air with a RH of 50% with (solid line) and without (dashed line) HONO (1.8 ppb). The markers in (a) indicate the NO signal at different temperatures ($[NO]_{640} = \square$, $[NO]_{450} = \diamond$, $[NO]_{amb} = \nabla$).

of HONO, respectively, and with a relative humidity of 50% and a CH_4 concentration of 1.7 ppm. In a rural setting (Fig. 7a), concentrations of NO_2 , ΣPN_s , ΣAN_s and HNO_3 each at 0.5 ppb for a total mixing ratio of NO_2 sources of 2 ppb, and of NO at 0.05 ppb would not be unusual (Day et al., 2003). The NO detected in the presence of 50 ppb of O_3 begins to rise above ambient at 250 °C due to the increasing importance of the reaction of NO_2 with atomic oxygen, peaks at 450 °C in the absence of HONO (dashed line) and at 640 °C in the presence of HONO (solid line). In the absence of HONO, the signal at 640 °C represents the sum of 80% of 0.05 ppb of ambient NO and 0.03 ppb of NO

produced by reducing NO_2 (1.5% of the total NO_2). A calculation with 100 ppt of HONO (solid line) shows that the total NO detected at 640 °C is 0.148 ppb. The NO difference with and without HONO is 78 ppt, almost exactly the expected 80% of the NO contained in the HONO. Fig. 7b depicts a situation that might be encountered in an urban center at night where O_3 is completely titrated by NO emissions that lead to high overall NO_x (70 ppb) and 2 ppb each of ΣPN_s , ΣAN_s and HNO_3 . Calculations show that in this situation, NO_2 reduction is eliminated and NO oxidation in the inlet would be only due to the RO_2 resulting from ΣPN_s and ΣAN_s dissociation. For this case, in the absence of HONO (dashed line), the NO signal at 640 °C (9.002 ppb) only has a contribution from the ambient NO. With the RO_2 contribution from ΣPN_s (2 ppb) and ΣAN_s (2 ppb) dissociation, approximately 90% of the ambient NO is detected after secondary chemistry. A calculation with 1.8 ppb of HONO which is 3% of the NO_2 mixing ratio (solid line) shows the total NO detected at 640 °C is 10.590 ppb, or an NO difference at 640 °C of 1.588 ppb, 88% of the HONO available.

4. Proposed configuration of a field instrument

The measurements described above show that (a) it is possible to detect and quantify HONO using TD-CL provided sufficient information about other trace gases (O_3 , H_2O and total NO_2 as defined above) is collected simultaneously and (b) our understanding of the most likely factors to affect the instrument response in the field is accurate. While this understanding, as represented in a model constrained by laboratory observations, is in our opinion essential to the success of the instrument, it would clearly be useful to further minimize and evaluate the effects of secondary chemistry directly in the field. Thus, for a field instrument we propose that the HONO response be directly evaluated by standard additions, that a three-channel instrument be employed to observe NO at ambient, 450 and 640 °C and that an improved inlet be implemented that reduces the effects of secondary chemistry. Note that the secondary chemical effects we describe as affecting the instrument response are not expected to vary with time. Thus, once they are characterized in the lab they can be treated as constants that depend only on concentrations of O_3 , H_2O , CH_4 and total NO_2 . The inlet in this instrument would be protected from sunlight to

avoid photolytic HONO production which has been observed by Zhou et al. (2002b). The first channel of the proposed three-channel instrument would be devoted to ambient NO detection, the second channel will measure the sum of HONO + NO via a 640 °C heated inlet and the third channel will be set at 450 °C to monitor the effects of secondary chemistry in the heated inlet due to the NO₂ + O reaction. To minimize secondary chemistry, we propose using an inlet modified from what we use above. A small orifice will be placed before the heating section resulting in a steep pressure drop to 300 torr. Quartz wool would not be used downstream of the heated section. Calculations of the performance of this modified inlet indicate that NO oxidation will be slower than in our laboratory prototype resulting in an NO detection efficiency of greater than 90% at O₃ of 100 ppb (compared to 80% for our prototype). The calculations also show that NO₂ reduction at 640 °C will be 1% of the total NO₂ at 100 ppb of O₃ (compared to 3% in our laboratory prototype). This makes the use of quartz wool downstream of the heated section unnecessary. We are currently unable to test this configuration of the inlet in the laboratory due to poor performance of our commercial NO detection system at low sample pressures. A custom built NO detector need not suffer from this limitation.

In summary, we developed and evaluated a lab prototype for in situ detection of HONO based on its TD to OH and NO followed by detection of the NO fragment by its CL reaction with O₃. We briefly describe modifications for using the technique to make field measurements of HONO. Evaluation of this technique under field conditions is required. In addition, it would be valuable to have a field intercomparison with the currently available technologies.

Acknowledgments

This work was supported by NASA under contract NAG5-13668 and NSF under contract ATM 0138669. I.M. Pérez gratefully acknowledges an NSF Graduate Research Fellowship.

Appendix A. Supplementary data

Supplementary data associated with this article can be found in the online version at [10.1016/j.atmosenv.2007.01.060](http://dx.doi.org/10.1016/j.atmosenv.2007.01.060).

References

- Alicke, B., Platt, U., Stutz, J., 2002. Impact of nitrous acid photolysis on the total hydroxyl radical budget during the limitation of oxidant production/Pianura Padana Produzione di Ozono study in Milan. *Journal of Geophysical Research—Atmospheres* 107, 8196.
- Alicke, B., Geyer, A., Hofzumahaus, A., Holland, F., Konrad, S., Pätz, H.W., Schäfer, J., Stutz, J., Volz-Thomas, A., Platt, U., 2003. OH formation by HONO photolysis during the BERLIOZ experiment. *Journal of Geophysical Research—Atmospheres* 108, 8247.
- Allegrini, I., Cortiello, M., Febo, A., Perrino, C., 1990. Generation of standard atmospheres of nitrous acid. In: *Physico-Chemical Behaviour of Atmospheric Pollutants*. Kluwer Academic Publishers, Dordrecht, pp. 140–144.
- Aumont, B., Chervier, F., Laval, S., 2003. Contribution of HONO sources to the NO_x/HO_x/O₃ chemistry in the polluted boundary layer. *Atmospheric Environment* 37, 487–498.
- Beine, H.J., Amoroso, A., Esposito, G., Sparapani, R., Ianniello, A., Georgiadis, T., Nardino, M., Bonasoni, P., Cristofanelli, P., Dominé, F., 2005. Deposition of atmospheric nitrous acid on alkaline snow surfaces. *Geophysical Research Letters* 32, L10808.
- Bertman, S., Marchewka, M., King, J., Weir, D., 2003. A method for measuring nitrous acid (HONO) flux using relaxed Eddy accumulation. *Eos Trans. AGU* 84(46) Fall Meeting supplement A32A-0131.
- Bytnerowicz, A., Sanz, M.J., Arbaugh, M.J., Padgett, P.E., Jones, D.P., Davila, A., 2005. Passive sampler for monitoring ambient nitric acid (HNO₃) and nitrous acid (HNO₂) concentrations. *Atmospheric Environment* 39, 2655–2660.
- Day, D.A., Wooldridge, P.J., Dillon, M.B., Thornton, J.A., Cohen, R.C., 2002. A thermal dissociation laser-induced fluorescence instrument for in situ detection of NO₂, peroxy nitrates, alkyl nitrates, and HNO₃. *Journal of Geophysical Research—Atmospheres* 107, 4046.
- Day, D.A., Dillon, M.B., Wooldridge, P.J., Thornton, J.A., Rosen, R.S., Wood, E.C., Cohen, R.C., 2003. On alkyl nitrates, O₃, and the “missing NO_y”. *Journal of Geophysical Research—Atmospheres* 108, 4501.
- Febo, A., Perrino, C., Gherardi, M., Sparapani, R., 1995. Evaluation of a high-purity and high-stability continuous generation system for nitrous-acid. *Environmental Science and Technology* 29, 2390–2395.
- Ferm, M., Sjödin, A., 1985. A sodium carbonate coated denuder for determination of nitrous acid in the atmosphere. *Atmospheric Environment* 19, 979.
- Finlayson-Pitts, B.J., Wingen, L.M., Sumner, A.L., Syomin, D., Ramazan, K.A., 2003. The heterogeneous hydrolysis of NO₂ in laboratory systems and in outdoor and indoor atmospheres: an integrated mechanism. *Physical Chemistry Chemical Physics* 5, 223–242.
- Genfa, Z., Slanina, S., Boring, B.C., Jongejan, P.A.C., Dasgupta, P.K., 2003. Continuous wet denuder measurements of atmospheric nitric and nitrous acids during the 1999 Atlanta Supersite. *Atmospheric Environment* 37, 1351–1364.
- Gormley, P.G., Kennedy, M., 1949. Diffusion from a stream flowing through a cylindrical tube. *Proceedings of the Royal Irish Academy Section A* 52, 163–169.
- Heland, J., Kleffmann, J., Kurtenbach, R., Wiesen, P., 2001. A new instrument to measure gaseous nitrous acid (HONO) in

- the atmosphere. *Environmental Science and Technology* 35, 3207–3212.
- Honrath, R.E., Lu, Y., Peterson, M.C., Dibb, J.E., Arsenaault, M.A., Cullen, N.J., Steffen, K., 2002. Vertical fluxes of NO_x , HONO, and HNO_3 above the snowpack at Summit, Greenland. *Atmospheric Environment* 36, 2629–2640.
- Kleffmann, J., Gavriloaiei, T., Hofzumahaus, A., Holland, F., Koppmann, R., Rupp, L., Schlosser, E., Siese, M., Wahner, A., 2005. Daytime formation of nitrous acid: a major source of OH radicals in a forest. *Geophysical Research Letters* 32, L05818.
- Liao, W., Hecobian, A., Mastromarino, J., Tan, D., 2006. Development of a photo-fragmentation/laser-induced fluorescence measurement of atmospheric nitrous acid. *Atmospheric Environment* 40, 17–26.
- Oms, M.T., Jongejan, P.A.C., Veltkamp, A.C., Wyers, G.P., Slanina, J., 1996. Continuous monitoring of atmospheric HCl, HNO_2 , HNO_3 , and SO_2 , by wet-annular denuder air sampling with on-line chromatographic analysis. *International Journal of Environmental Analytical Chemistry* 62, 207–218.
- Ren, X., Harder, H., Martinez, M., Leshner, R.L., Olinger, A., Simpas, J.B., Brune, W.H., Schwab, J.J., Demerjian, K.L., He, Y., Zhou, X., Gao, H., 2003. OH and HO_2 chemistry in the urban atmosphere of New York City. *Atmospheric Environment* 37, 3639–3651.
- Ridley, B.A., Grahek, F.E., 1990. A small, low flow, high-sensitivity reaction vessel for no chemiluminescence detectors. *Journal of Atmospheric and Oceanic Technology* 7, 307–311.
- Rosen, R.S., 2004. Observations of NO_2 , peroxy nitrates, alkyl nitrates, HNO_3 and total NO_y in Houston, TX: implications for O_3 photochemistry, Ph.D. dissertation. University of California, Berkeley, CA.
- Simon, P.K., Dasgupta, P.K., 1995. Continuous automated measurement of gaseous nitrous and nitric-acids and particulate nitrite and nitrate. *Environmental Science and Technology* 29, 1534–1541.
- Stutz, J., Alicke, B., Ackermann, R., Geyer, A., Wang, S., White, A.B., Williams, E.J., Spicer, C.W., Fast, J.D., 2004. Relative humidity dependence of HONO chemistry in urban areas. *Journal of Geophysical Research—Atmospheres* 109, D03307.
- Takenaka, N., Terada, H., Oro, Y., Hiroi, M., Yoshikawa, H., Okitsu, K., Bandow, H., 2004. A new method for the measurement of trace amounts of HONO in the atmosphere using an air-dragged aqua-membrane-type denuder and fluorescence detection. *Analyst* 129, 1130–1136.
- Večeřa, Z., Dasgupta, P.K., 1991. Measurement of ambient nitrous-acid and a reliable calibration source for gaseous nitrous-acid. *Environmental Science and Technology* 25, 255–260.
- Wang, L., Zhang, J., 2000. Detection of nitrous acid by cavity ring down spectroscopy. *Environmental Science and Technology* 34, 4221–4227.
- Zellweger, C., Ammann, M., Hofer, P., Baltensperger, U., 1999. NO_y speciation with a combined wet effluent diffusion denuder-aerosol collector coupled to ion chromatography. *Atmospheric Environment* 33, 1131–1140.
- Zhou, X.L., Qiao, H.C., Deng, G.H., Civerolo, K., 1999. A method for the measurement of atmospheric HONO based on DNPH derivatization and HPLC analysis. *Environmental Science and Technology* 33, 3672–3679.
- Zhou, X.L., Civerolo, K., Dai, H.P., Huang, G., Schwab, J., Demerjian, K., 2002a. Summertime nitrous acid chemistry in the atmospheric boundary layer at a rural site in New York State. *Journal of Geophysical Research—Atmospheres* 107, 4590.
- Zhou, X.L., He, Y., Huang, G., Thornberry, T.D., Carroll, M.A., Bertman, S.B., 2002b. Photochemical production of nitrous acid on glass sample manifold surface. *Geophysical Research Letters* 29, L015080.